Missouri University of Science and Technology

Scholars' Mine

Electrical and Computer Engineering Faculty Research & Creative Works

Electrical and Computer Engineering

01 Jan 2023

Transformer Leakage Inductance Design Methodology

Angshuman Sharma

Jonathan W. Kimball

Missouri University of Science and Technology, kimballjw@mst.edu

Follow this and additional works at: https://scholarsmine.mst.edu/ele_comeng_facwork

 Part of the Electrical and Computer Engineering Commons

Recommended Citation

A. Sharma and J. W. Kimball, "Transformer Leakage Inductance Design Methodology," *Conference Proceedings - IEEE Applied Power Electronics Conference and Exposition - APEC*, pp. 1572 - 1578, Institute of Electrical and Electronics Engineers, Jan 2023.

The definitive version is available at https://doi.org/10.1109/APEC43580.2023.10131409

This Article - Conference proceedings is brought to you for free and open access by Scholars' Mine. It has been accepted for inclusion in Electrical and Computer Engineering Faculty Research & Creative Works by an authorized administrator of Scholars' Mine. This work is protected by U. S. Copyright Law. Unauthorized use including reproduction for redistribution requires the permission of the copyright holder. For more information, please contact scholarsmine@mst.edu.

Transformer Leakage Inductance Design Methodology

Angshuman Sharma and Jonathan W. Kimball
Department of Electrical and Computer Engineering
Missouri University of Science and Technology
Rolla, MO USA
Email: asc4v@mst.edu, kimballjw@mst.edu

2023 IEEE Applied Power Electronics Conference and Exposition (APEC) | 978-1-6654-7539-6/23/$31.00 ©2023 IEEE | DOI: 10.1109/APEC43580.2023.10131409

***Abstract*—The leakage inductance exhibited by a transformer depends on its winding geometry, which generally involves the selection of several key design parameters in addition to the winding structure and the interleaving configuration. With few resources explaining the effects of these design choices on the observed leakage inductance, numerous trial-and-error iterations become necessary to realize the desired leakage inductance. This paper explores more than a hundred winding geometries feasible in a 2-winding transformer comprising the same magnetic core, number of turns, and wire gauge, and finds the leakage inductance for each unique design using 2-D finite element method (FEM) simulations in association with the semi-analytical double-2-D model. These leakage inductances are plotted and further analyzed to understand the effects of different design parameters on the effective leakage inductance. The results presented herein and the conclusions drawn from this research can serve as a valuable resource for future design practitioners from both industry and academia.**

***Index Terms*—Double-2-D model, finite element method (FEM), leakage inductance, transformer.**

I. Introduction

Transformers are an integral part of power electronic converters where galvanic isolation is a prerequisite besides level shifting of voltages [1]. Lately, transformers with integrated magnetics have gained a lot of attention from the power electronics community. The leakage inductance of these transformers has the capability to replace the series inductor of the converter if designed appropriately. This scope to reduce cost and footprint has fuelled the demand for these transformers for an efficient power conversion process [2, 3, 4].

Designing a magnetically-integrated transformer that meets the desired series inductance is a two-step process. The first step involves the general design procedure that is common to any transformer. Here, the Area Product Method can be used to find the required core, number of turns, and wire gauge for a naturally air-cooled transformer [5, 6]. The second step involves an iterative process where different feasible winding geometries are tried and tested until the leakage inductance matches the desired series inductance [7].

The leakage inductance of a transformer is the byproduct of the magnetic energy stored in the 3-D space in and around the transformer [2, 8]. For the same magnetic core and number of turns, the amount of stored energy depends on the selected winding structure and the interleaving configuration in addition to some key design parameters, like

1) air gap between primary and secondary winding layers (inter-winding gap),
2) air gap between two layers of the same winding (inter-layer gap),
3) air gap between two turns within a layer (inter-turn gap), and
4) overlapping height of the two windings.

A clear understanding of the outcome of these design choices is found to be critical for an efficient design process. While the handbooks on transformer designs share no light on this additional design step [5, 6], the existing literature on leakage inductance calculation methods falls short in deciphering the effects of these design choices on the observed leakage inductance [9]. As a result, numerous trial-and-error iterations become necessary to achieve the desired leakage inductance. This paper attempts to bridge this existing knowledge gap and make the design process of magnetically-integrated transformers simpler and more efficient.

The paper begins with the general design of a magnetically-integrated transformer targeted for an isolated resonant dc-dc converter, where matching the desired series resonant inductance can be pivotal to the optimal operation of the converter. Using the same magnetic core, number of turns, and wire gauge, section 3 explores more than a hundred feasible winding geometries and finds the leakage inductance for each unique design. Section 4 presents and analyzes the results. Section 5 provides guidance to enable future designers to realize the desired leakage inductance of any transformer more efficiently. The paper finally ends with a concluding remark.

II. General Transformer Design

Table I shows the specifications of a naturally air-cooled 2-winding transformer for an isolated resonant dc-dc converter. Here, the Area Product Method is used to find the required magnetic core, number of turns, and wire gauge. The area product A_p (in cm^4) which indicates the power handling capability of a transformer can be calculated using,

$$A_p = \left(\frac{S_{tot}(10^4)}{K_u K_f K_j B_{max} f} \right)^{(8/7)} \tag{1}$$

$$S_{tot} = \sqrt{2}\big(V_1 I_1 + V_2 I_2\big) \tag{2}$$

Authorized licensed use limited to: Missouri University of Science and Technology. Downloaded on August 16,2023 at 17:40:20 UTC from IEEE Xplore. Restrictions apply.

TABLE I
TRANSFORMER SPECIFICATIONS

Output power	1 kVA
Input voltage (rms)	340 V
Turns ratio	1
Operating frequency	220 kHz
Duty cycle	0.5
Maximum flux density	0.1 T
Maximum temperature rise	50° C

where S_{tot} is the total apparent power (in VA), K_u is the window fill factor, K_f is the waveform coefficient, and K_j is the temperature-rise constant. Here, it is assumed that $K_u = 0.35$, $K_f = 4.44$ for sinusoidal currents, and $K_j = 534$ for the target ferrite EE core to stay below the specified temperature rise limit. The magnetic core selected to construct the transformer should satisfy $W_a A_c \geq A_p$, where the area product $W_a A_c$ can be obtained from the datasheet of the core. The number of primary turns needed to operate the transformer can be calculated using Faraday's law,

$$N_1 = \frac{V_1(10^4)}{K_f B_{max} f A_c} \tag{3}$$

where A_c is the cross-sectional area of the core (in cm^2). N_1 should be a natural number. Finally, the peak current density (in A/cm^2) inside the winding window of the selected core can be calculated using,

$$J = \frac{S_{tot}(10^4)}{K_u K_f B_{max} f (W_a A_c)} \tag{4}$$

The current density of the selected wire gauge should be less than J calculated in (4) to meet the specified temperature rise limit. Table 2 summarizes the results of the Area Product Method. Two ETD 39 cores from EPCOS with the corresponding bobbin and AWG 19 enameled copper wire are selected to construct the transformer. The formulations for other parameters like core and copper losses and temperature rise can be found in [6, 10].

III. LEAKAGE INDUCTANCE DESIGN

The leakage inductance of a transformer depends on its winding geometry, as explained in section I. For the selected core, number of turns, and wire gauge, the two most popular winding structures seen in 2-winding EE-core transformers are depicted in Figs. 1 (a) and (b), where the secondary winding is either wound over or below the primary winding [8]. In the first structure, the 40 turns per winding are arranged in two layers of 20 turns each. The two primary (P) and secondary (S) layers can then be arranged in three unique interleaving configurations—PPSS as represented in Fig. 1 (a), PSPS as represented in Fig. 1 (c), and PSSP as represented in Fig. 1 (d). In the second P-S structure, the 40 turns per winding are arranged in 8 layers of 5 turns each. Interleaving is feasible but not pursued to avoid redundancy.

For a particular winding structure and interleaving configuration, the leakage inductance again depends on four critical

TABLE II
RESULTS OF THE AREA-PRODUCT METHOD

Minimum area product	1.65 cm^4
Selected core	ETD 39 ($WaAc = 2.18$ cm^4)
Peak current density	484 A/cm^2
Selected wire gauge	AWG 19 ($J = 450$ A/cm^2)
Primary turns	40
Secondary turns	40
Core loss	1.27 W
DC copper loss	1.24 W
Temperature rise	34.9° C
DC Efficiency	99.75 %

TABLE III
IDEAL VALUES OF DIFFERENT PARAMETERS

Parameter	Value (mm)			
	PPSS	PSPS	PSSP	P-S
d_l	0.2	0.2	0.2	0.2
d_w	0.2	0.2	0.2	0.3
d_t	0.1	0.2	0.2	0.2
d_g	0	1.8	1.8	0

design parameters: inter-winding gap d_w, inter-layer gap d_l, inter-turn gap d_t, and height offset d_g, as indicated in Fig. 1. Sweeping these parameters within their reasonable range can result in countless winding geometries and as many leakage inductances. In order to study these geometries, a core with 30 % larger area product is chosen. For the four structures in Fig. 1, the ideal values of different parameters are presented in Table III. Unless specified, these parameters assume the given values. Fig. 2 shows the magnetomotive force (MMF) distribution in these structures, where the MMF is constant across the inter-layer and inter-winding gaps and linearly varying across the winding cross-sections.

In this paper, the leakage inductances are evaluated using 2-D finite element model (FEM) simulations in association with the double-2-D model [2] to reduce computation time. At first, the inside window (IW) and the outside window (OW) planes of each transformer are modeled in COMSOL Multiphysics to find the magnetic energy per unit length E' across these planes. Then E' is scaled to find the leakage inductance per unit length $L' = 2E'/I_1^2$ across each plane, where I_1 is the primary current. Finally, the leakage inductance is calculated using the semi-analytical double-2-D model, given by

$$L_{lk,\text{double-2-D}} = s_c \left(L'_{(\text{IW})} d_{(\text{IW})} + L'_{(\text{OW})} d_{(\text{OW})} \right) \tag{5}$$

$$s_c = \begin{cases} 1, & \text{core-type transformer} \\ 2, & \text{shell-type transformer} \end{cases}$$

where d is the partial leakage length. Fig. 3 illustrates the concept of the double-2-D model for core-type (UU and UI core-type) and shell-type (EE and EI core-type) transformers, where l is the leakage radius obtained by averaging E' across the planes, and θ is the leakage angle. For EE cores with a circular winding leg having a radius r_c, the leakage

Authorized licensed use limited to: Missouri University of Science and Technology. Downloaded on August 16,2023 at 17:40:20 UTC from IEEE Xplore. Restrictions apply.

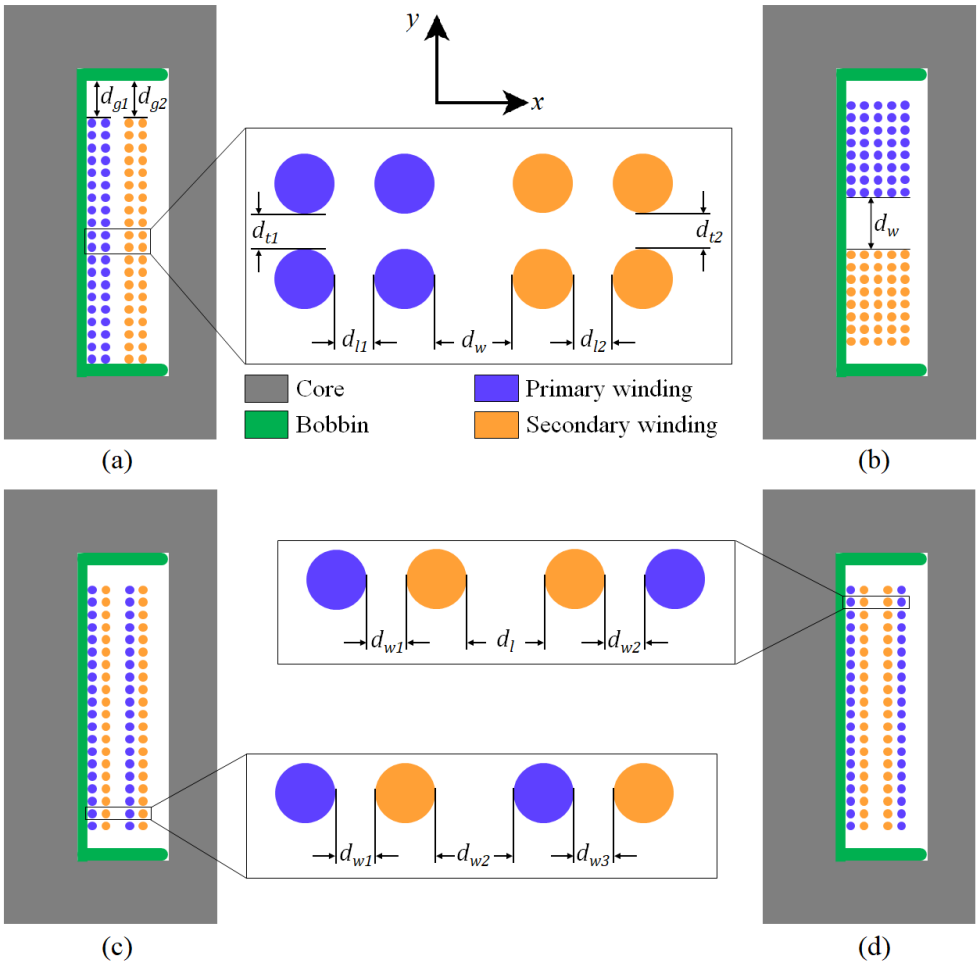

Fig. 1. Winding structures: (a) PPSS, (b) P-S, (c) PSPS, (d) PSSP.

angles across the IW, OW and transition (TR) regions can be calculated using,

$$\theta_{(\mathrm{IW})} = 2\arcsin\left(\frac{r_c}{w + r_c}\right) \tag{6}$$

$$\theta_{(\mathrm{TR})} = \arcsin\left(\frac{2r_c}{l_{(\mathrm{IW})} + l_{(\mathrm{OW})}}\right) - \frac{\theta_{(\mathrm{IW})}}{2} \tag{7}$$

$$\theta_{(\mathrm{OW})} = \frac{2\pi - s_c(\theta_{(\mathrm{IW})} + 2\theta_{(\mathrm{TR})})}{s_c} \tag{8}$$

where w is the width of the IW plane. Finally, the partial leakage lengths can be calculated using,

$$d_{(\mathrm{IW})} = l_{(\mathrm{IW})}\big(\theta_{(\mathrm{IW})} + \theta_{(\mathrm{TR})}\big) \tag{9}$$

$$d_{(\mathrm{OW})} = l_{(\mathrm{OW})}\big(\theta_{(\mathrm{OW})} + \theta_{(\mathrm{TR})}\big) \tag{10}$$

Detailed mathematical formulations of the double-2-D model can be found in [2]. High-frequency analysis of the leakage inductance is avoided in light of multi-strand litz wires.

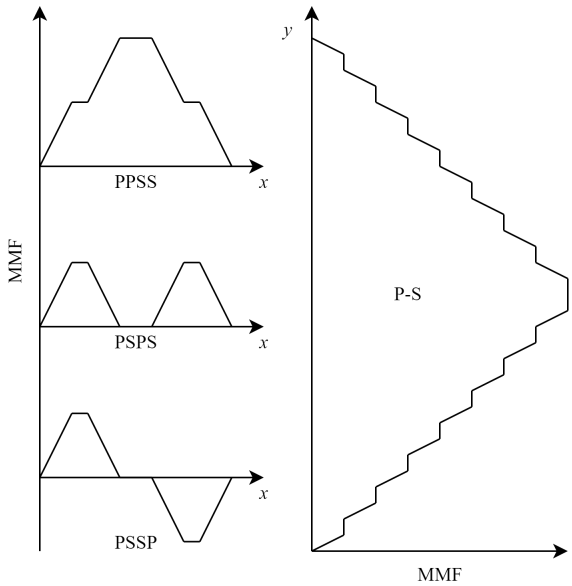

Fig. 2. MMF distribution in different structures.

Authorized licensed use limited to: Missouri University of Science and Technology. Downloaded on August 16,2023 at 17:40:20 UTC from IEEE Xplore. Restrictions apply.

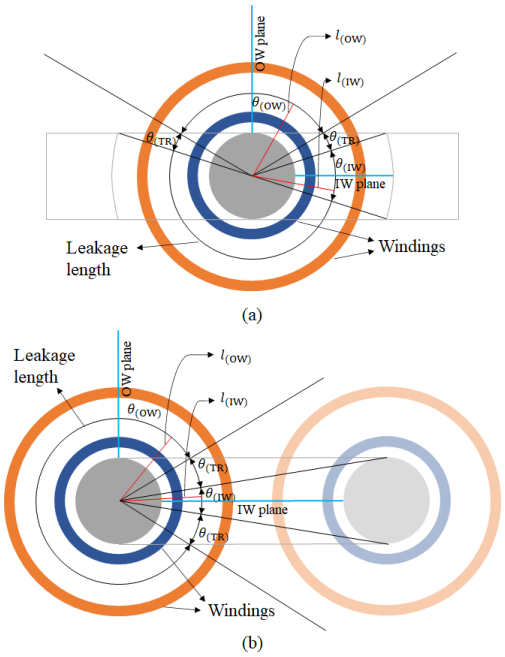

Fig. 3. Double-2-D model: (a) shell-type transformer, (b) core-type transformer [2].

IV. Results

Figs. 4, 5 and 6 plot the leakage inductances resulting from the parametric sweeps performed on the PPSS structure. On the other hand, Figs. 8, 9 and 10 plot the leakage inductances corresponding to the parametric sweeps performed on the PSPS, PSSP and P-S structures, respectively. Detailed discussions of these plots are provided in the following subsections. Additionally, for each winding structure, the FEM-generated magnetic energy density across the IW plane assuming the ideal parameter values in Table III is shown in Fig. 11.

A. PPSS structure

In Fig. 4, the leakage inductance increases very linearly with d_{l1}, d_{l2} and d_w because of the constant, non-zero MMFs across these air gaps and a linear increase in the leakage radii. The increase in leakage inductance with d_{l1} or d_{l2} is similar but much lower than that with d_w because the MMFs across d_{l1} and d_{l2} are similar but lower than that across d_w, as seen in Fig. 2. If all three air gaps are increased equally, then the net increase in leakage inductance follows a slope that is equivalent to the sum of the slopes of the first three curves.

In Fig. 5, an equal increase in d_{t1} and d_{t2} decreases the leakage inductance because of a reduction in magnetic energy density in the inter-turn gaps as the windings start spreading out along the layers. An equal change in d_{g1} and d_{g2} hardly affects the leakage inductance, as seen in Fig. 6. However, increasing d_{g1} only increases the leakage inductance somewhat quadratically. This increase is entirely due to the increase in the radial component of magnetic field intensity, which otherwise is negligible when there is a complete overlap between the two winding heights.

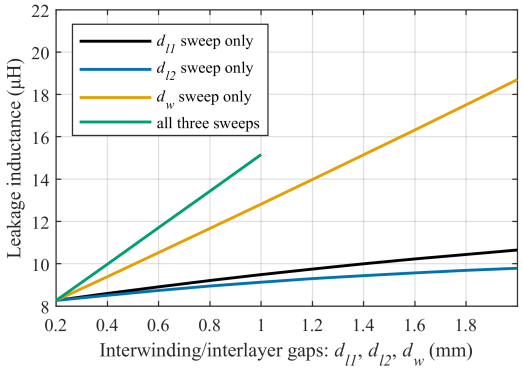

Fig. 4. Variation of d_{l1}, d_{l2} and d_w in PPSS.

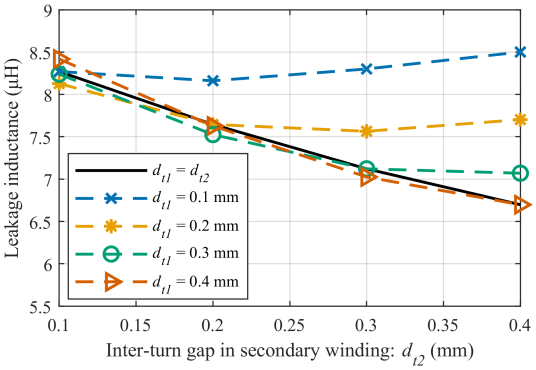

Fig. 5. Variation of d_{t1} and d_{t2} in PPSS.

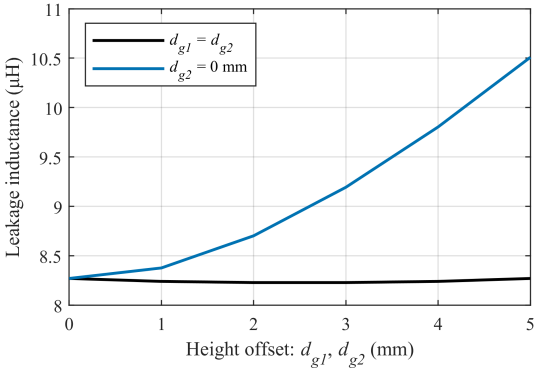

Fig. 6. Variation of d_{g1} and d_{g2} in PPSS.

B. PSPS structure

In Fig. 8, the increase in leakage inductance with d_{w1} or d_{w3} is similar and almost linear. This is because the MMFs across d_{w1} and d_{w3} are equal, constant and non-zero, and the increase in leakage radii with d_{w1} or d_{w3} is also linear. The increase in leakage inductance with d_{w2} is trivial because the MMF across d_{w2} is negligible and the small increase in leakage inductance is a result of the increase in leakage radii only. If all three air gaps are increased equally, the net increase in leakage inductance is very linear and it follows a slope that is equivalent to the sum of the slopes of the first three curves.

Authorized licensed use limited to: Missouri University of Science and Technology. Downloaded on August 16,2023 at 17:40:20 UTC from IEEE Xplore. Restrictions apply.

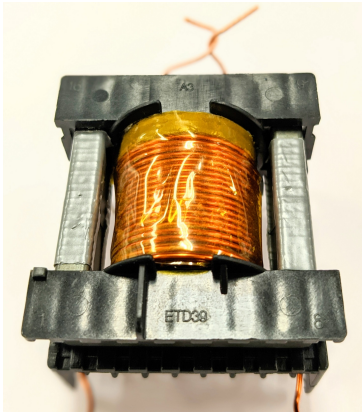

Fig. 7. Experimental prototype of the transformer with PPSS winding structure.

C. PSSP structure

In Fig. 9, the increase in leakage inductance with d_{w1} or d_{w2} is very linear and identical because the MMFs across d_{w1} and d_{w2} are equal, constant and non-zero. The increase in leakage radii with d_{w1} or d_{w2} is also linear. As expected, the small increase in leakage inductance with d_l is due to the increase in leakage radii only. Similar to the PSPS structure, if all three air gaps are increased equally, the net increase in leakage inductance is linear and it follows a slope that is equivalent to the sum of the slopes of the first three curves.

D. P-S structure

In Fig. 10, the leakage inductance increases almost linearly with d_w because the MMF across d_w is constant and non-zero. This case is somewhat similar to sweeping d_w in the PPSS structure. Since the P-S structure has 8P-8S uninterleaved layers, the MMF across d_w is very high, as seen in Fig. 2, thereby resulting in a steep increase in the leakage inductance. The leakage radii, however, remain constant. Saturation may show up when d_w is very large.

E. Experimental results

To demonstrate the efficacy of the leakage inductance design and calculation method explained in section III, an experimental prototype of the PPSS structured transformer is built in the lab. The measured leakage inductance is found to be $8.3\,\mu$H compared to the simulated value of $8.27\,\mu$H.

V. Discussion

Results presented herein restate the fact that the leakage inductance of a transformer depends on its winding geometry. Ideally, there can be countless possibilities to wind a transformer, but not all winding geometries will result in the desired leakage inductance. Unfortunately, there is no mathematical formulation to reach the desired leakage inductance in a single step. Hence, a few iterations may be essential to find the appropriate winding geometry. Nevertheless, to make future leakage inductance designs simpler and more efficient, some key observations from this research are provided below:

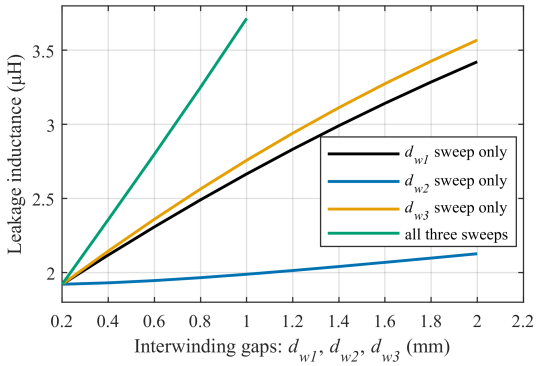

Fig. 8. Variation of d_{w1}, d_{w2} and d_{w3} in PSPS.

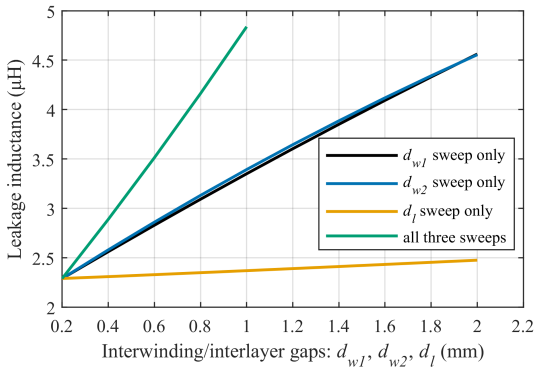

Fig. 9. Variation of d_{w1}, d_{w2} and d_l in PSSP.

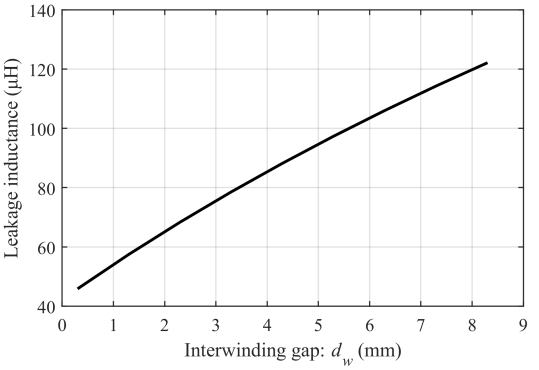

Fig. 10. Variation of d_w in P-S.

1) Interleaving of layers can reduce the effective leakage inductance significantly.
2) Alternately arranged P and S layers typically give the smallest leakage inductance.
3) For higher leakage inductance, it is more important to have more layers comprising fewer conductors than fewer layers comprising more conductors.
4) Selecting a larger core provides more room for adjusting the different gaps when a large leakage inductance is in demand.
5) Most of the leakage energy is stored in the inter-winding gap; so varying this gap can help in making any large

Authorized licensed use limited to: Missouri University of Science and Technology. Downloaded on August 16,2023 at 17:40:20 UTC from IEEE Xplore. Restrictions apply.

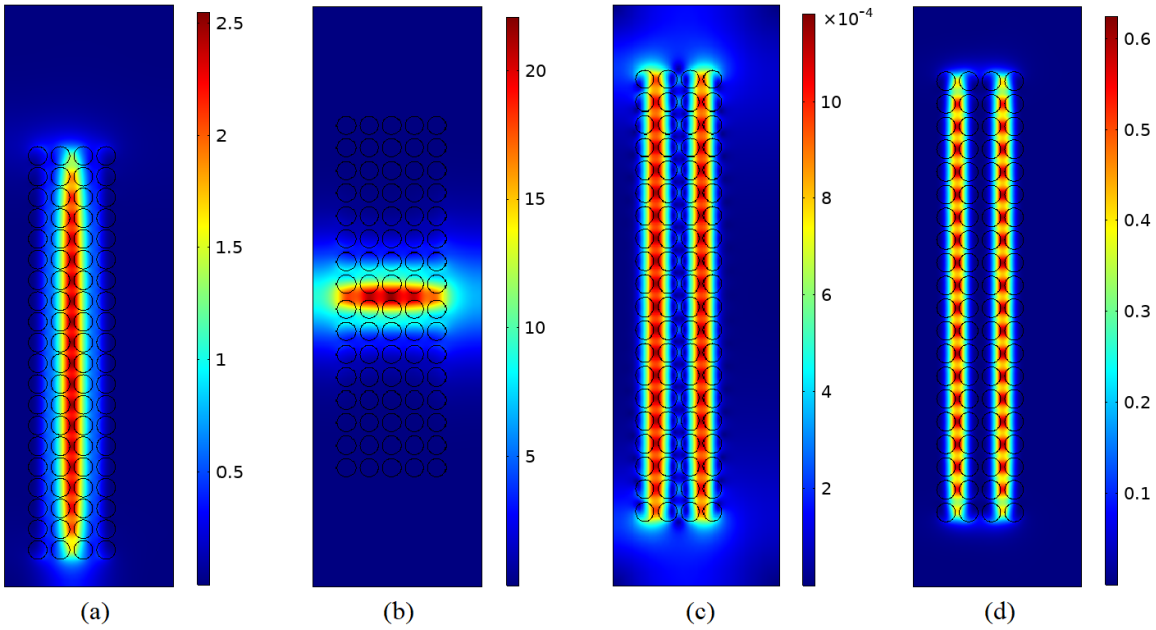

Fig. 11. Magnetic energy density ($\mathrm{J/m^3}$) in the transformer winding window: (a) PPSS, (b) P-S, (c) PSPS, (d) PSSP.

adjustments in the leakage inductance.

6) The leakage inductance varies linearly with the inter-winding gap.
7) The increase in leakage inductance is very linear and notable when all inter-layer and inter-winding gaps are increased by the same amount.
8) Offsetting the height of one of the windings can also increase the leakage inductance.
9) For small adjustments, changing the inter-turn gap can help if done for both windings.
10) For the smallest adjustments, the inter-layer gap can be modified.

VI. Conclusion

In this paper, a 1 kVA, 340/340 V, 220 kHz, 2-winding transformer with integrated magnetics is designed for a resonant dc-dc converter using the Area Product Method. Two ETD 39 ferrite cores and 40 turns of enameled AWG 19 wires per winding are selected for constructing the transformer. Since the leakage inductance depends on the winding geometry, four different winding structures including three interleaved configurations are explored. Results show that with the same ferrite core, number of turns, and wire gauge, a leakage inductance between 1.9 and 122.1 µH is achievable—a span of almost two orders of magnitude. One of the winding structure is also modeled experimentally. Additionally, four key design parameters are investigated. Sweeping these parameters across their respective range shows fascinating trends in the effective leakage inductance. These observations are recorded to help future design practitioners in realizing the desired leakage inductance with fewer trial-and-error iterations.

Acknowledgment

This material is based upon work supported by the Department of Energy Vehicle Technologies Office under Award Number DE-EE0008449. This report was prepared as an account of work sponsored by an agency of the United States Government. Neither the United States Government nor any agency thereof, nor any of their employees, makes any warranty, express or implied, or assumes any legal liability or responsibility for the accuracy, completeness, or usefulness of any information, apparatus, product, or process disclosed, or represents that its use would not infringe privately owned rights. Reference herein to any specific commercial product, process, or service by trade name, trademark, manufacturer, or otherwise does not necessarily constitute or imply its endorsement, recommendation, or favoring by the United States Government or any agency thereof. The views and opinions of authors expressed herein do not necessarily state or reflect those of the United States Government or any agency thereof.

References

[1] A. Sharma and S. Sharma, "Review of power electronics in vehicle-to-grid systems," *Journal of Energy Storage*, vol. 21, pp. 337–361, 2019.
[2] A. Sharma and J. W. Kimball, "Evaluation of transformer leakage inductance using magnetic image method," *IEEE Transactions on Magnetics*, vol. 57, no. 11, pp. 1–12, 2021.
[3] A. Sharma and J. W. Kimball, "Novel transformer with variable leakage and magnetizing inductances," in *2021 IEEE Energy Conversion Congress and Exposition (ECCE)*. IEEE, 2021, pp. 2155–2161.
[4] A. Sharma, K. J. Veeramraju, and J. W. Kimball, "Power flow control of a single-stage ac-ac solid-state transformer for ac distribution system," in *2022 IEEE Power and Energy Conference at Illinois (PECI)*. IEEE, 2022, pp. 1–6.
[5] R. W. Erickson and D. Maksimovic, *Fundamentals of power electronics*. Springer Science & Business Media, 2007.
[6] C. W. T. McLyman, *Transformer and inductor design handbook*. CRC press, 2004.

Authorized licensed use limited to: Missouri University of Science and Technology. Downloaded on August 16,2023 at 17:40:20 UTC from IEEE Xplore. Restrictions apply.

[7] Z. Ouyang, O. C. Thomsen, and M. A. Andersen, "The analysis and comparison of leakage inductance in different winding arrangements for planar transformer," in *2009 International Conference on Power Electronics and Drive Systems (PEDS)*. IEEE, 2009, pp. 1143–1148.
[8] M. S. S. Nia, P. Shamsi, and M. Ferdowsi, "Investigation of various transformer topologies for hf isolation applications," *IEEE Transactions on Plasma Science*, vol. 48, no. 2, pp. 512–521, 2020.
[9] R. Schlesinger and J. Biela, "Comparison of analytical models of transformer leakage inductance: Accuracy versus computational effort," *IEEE Transactions on Power Electronics*, vol. 36, no. 1, pp. 146–156, 2020.
[10] R. Ridley and A. Nace, "Modeling ferrite core losses," *Switching Power Magazine*, vol. 3, no. 1, pp. 6–13, 2002.

Authorized licensed use limited to: Missouri University of Science and Technology. Downloaded on August 16,2023 at 17:40:20 UTC from IEEE Xplore. Restrictions apply.